Title	Attenuation Property of Coda Parts of Seismic Waves from Local Earthquakes
Author(s)	AKAMATSU, Junpei
Citation	Bulletin of the Disaster Prevention Research Institute (1980), 30(1): 1-16
Issue Date	1980-07
URL	http://hdl.handle.net/2433/124890
Right	
Type	Departmental Bulletin Paper
Textversion	publisher

Attenuation Property of Coda Parts of Seismic Waves from Local Earthquakes

By Junpei AKAMATSU

(Manuscript received April 1, 1980)

Abstract

Coda parts of the seismic waves from local earthquakes occurring in the Kinki district were analyzed to discuss the mechanisms of generation and attenuation of the coda waves. The attenuation and fluctuation of the logarithmic rms amplitudes of the band-pass filtered traces ranging from 1 to 20 HZ are characterized as follows; The decay curve of each band is well fitted to the functional form of the lapse time t measured from source origin time, $t^{-a}e^{-bt}$. The geometrical spreading factor a is $1\sim2$ for the intervals $15\sim300$ sec in each frequency band. The attenuation coefficient b depends on the frequency as well as the lapse time. When the lapse time is early ($t<50$ sec), the Q values derived from b under the condition where $a=1$ are 150 at 1 HZ and 780 at 16 HZ, while they increase to 210 at 1 HZ and 1000 at 16 HZ, respectively, for the large lapse time ($t>50$ sec). In each time interval the dependence of the Q values on frequency is remarkable. The turbidity coefficient derived from the fluctuation of amplitudes is rather constant for frequency, but decreases with time similarly to the attenuation property, showing the vertical variation of turbidity in the earth.

1. Introduction

Recently coda parts of seismograms have arisen seismological interests as scattered waves caused by randomly distributed heterogeneities in the earth. Total duration time of a seismogram has been used as a measure of magnitude for local earthquakes because of its independence of the epicentral distance[1),2)]. The level of coda amplitude and its attenuation property are studied to investigate the seismic moment and spectra of the earthquake source, and the parameters of attenuation in the medium and their regional variation[3)-8)].

In the course of a study of the coda parts of seismograms, it is usually accepted that the waves of coda parts are generated by scattering caused by heterogeneities in the medium[9)]. The most important characteristics of seismic coda are as follows; it depends not only on the fine structures on the direct wave path from source to station but also on the physical properties of the layers in which the scattered waves may propagate; it depends not only on the radiation of the direction from source to station but also on the mean effect of the radiation from all directions; it does not depend on the epicentral distance as long as the lapse time measured from the source origin time is sufficiently great. Many observations have confirmed the above conception.

The decay curve of the observed coda is assumed to converge to the asymptotic decay curve which should be observed at the source region, when the lapse time t is 2–3 times larger than the travel time of S wave t_s ($t>2$–$3\cdot t_s$)[10)]. The decay of the asymptote, idealized for a general decay form of observed coda, is predicted with a

few different physical models having the same functional form of $t^{-a}e^{-bt}$. The geometrical spreading facter a is 1 for the single scattering model of body waves or 0.5 for surface ones, and 0.75 for the diffusion model. The attenuation coefficient b will depend on the absorption of the medium and on the fractional loss of energy by wave scattering. The Q value, calculated with an assumption of some scattering model, for example $a=1$, shows strong dependency on frequency with a simple functional relation in the frequency range of 0.1–50 Hz[8),9)]. On the contrary, some variability is indicated by the Q data derived from analyses of body and surface waves[11,12)].

The attenuation property of the seismic coda has been discussed with a general decay curve constructed by ensemble of many envelopes of peak amplitudes of coda parts[8)] or manually smoothed decay curves[3),7)]. These procedures may introduce some difference in the time intervals used for analysis for different frequency bands.

The coda part of a seismogram is characterized by some amount of fluctuation of amplitude, which may be caused by the scattering effects of seismic waves and is interesting in connection with the problem of generation of seismic coda.

In view of the above the attenuation and fluctuation properties of coda parts of local small earthquakes which occurred in the Kinki district are studied with the rms amplitude made by means of the integrators of ac meters.

2. Analysis of data

Local small earthquakes with magnitudes from 2.3 to 4.9 (JMA) were analyzed. These were observed with the analog magnetic recording system operated routinely at the Sumiyama Seismic Station of the Disaster Prev. Res. Inst. of Kyoto University in the southern part of Kyoto prefecture. The hypocentral distances Δ of almost all of the events are less than 100 km, although events with larger Δ (100~200 km) are analyzed for a comparative study (Fig. 1). The focal depths H range up to 70 km. However, the depths vary with the source regions as seen in Fig. 1. The analyzed events are grouped with their source regions and are listed in Table 1, in which the hypocentral distances Δ and azimuths φ are calculated with the source locations of JMA data.

The two different recording ranges of the observational system are available to increase the dynamic recording range; 7.7~770 μ kine for the high gain channels and 96 μ~9.6 m kine for the low gain. To examine the dependence of the characteristics of the coda on frequency the five band pass filters are used, the center frequencies f_0 of which are 1, 2, 4, 8 and 16 HZ, respectively, with band width $\sqrt{2}f_0$ as shown in Fig. 2.

The outputs of each filter are converted to dc levels with the ac meters to generate the rms amplitudes $A(f, t)$, which are digitized with sampling intervals of 0.5 sec. Fig. 3 shows the circuit diagram and the response curves of sinusoidal inputs. The averaging time constant T selected are 10 sec for the band width $f_0=1$ HZ, and 5 sec for $f_0 \geq 2$ HZ. The examples of filtered traces and rms amplitudes $A(f, t)$ are shown in Fig. 4.

As is mentioned in the preceding section the rms amplitude $A(f, t)$ will take the following general form of attenuation of coda for the large lapse time t;

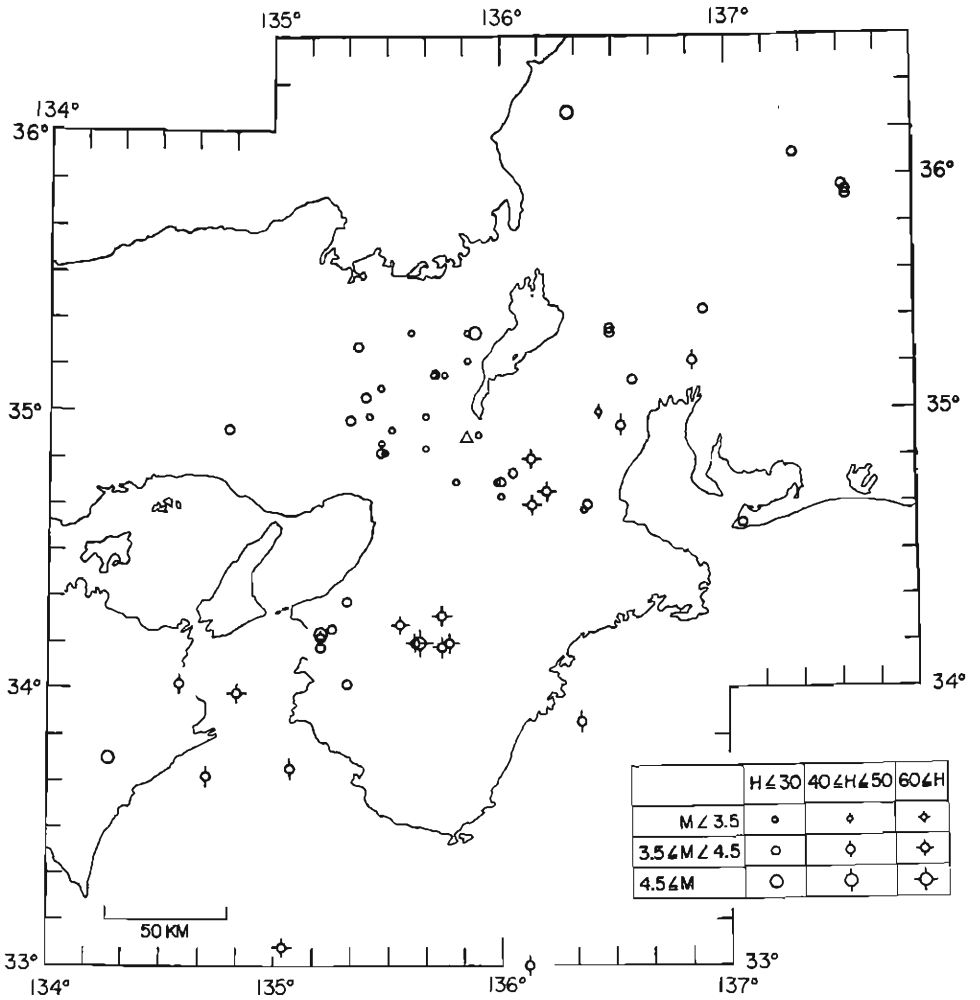

Fig. 1. Epicenters of analyzed earthquakes. △ denotes the Sumiyama Seismic Station.

$$A(f, t)=c\,t^{-a}e^{-bt} \tag{1}$$

where c represents the coda source factor[3]. Taking the logarithm of both sides in Eq. (1), we obtain

$$\ln A(f, t)=C-a\ln t-bt. \tag{2}$$

The coefficients a, b and C in Eq. (2) are calculated with each $\ln A(f, t)$ of the events separately by the method of least square. The analyzed time interval t for each $A(f, t)$ is defined by $3\,t_s\leq t\leq t_{3\cdot s/N}$, where t_s denotes the travel time of the direct S wave and $t_{3\cdot s/N}$ is the time when the amplitude $A(f, t)$ becomes smaller than the 3 times level of the noise before and after the event in each channel. With these time intervals the data points of every 5 seconds for $A(f_0=1, t)$ or 2.5 seconds for $A(f_0\geqq 2, t)$ are used for calculation of the least square, that is, two data points are

Table 1. List of the Earthquakes Analyzed

No.	Event No.	Date	Time h m	Distance km	Azimuth N °E	Depth km	Magnitude	Region
1	76– 264*	Sept. 14 1976	21 42	57	−50	10	4.2	Central Kyoto Pref.
2	76– 496	Nov. 13 1976	21 29	34	−72	10	3.3	Central Kyoto Pref.
3	77– 431	July 27 1977	15 04	42	0	20	2.9	Westarn Shiga Pref.
4	77– 678	Aug. 23 1977	17 38	18	−62	20	3.2	Near Kyoto
5	77–1316	Nov. 25 1977	12 53	44	−68	10	3.8	Kyoto-Osaka Border
6	78– 24*	Jan. 7 1978	6 01	47	−81	10	4.0	Eastern Hyogo Pref.
7	78– 604	June 13 1978	2 07	30	−94	10	2.8	Kyoto-Osaka Border
8	78– 656	June 29 1978	19 32	5	76	10	2.8	Sw Shiga Pref.
9	78– 731	July 29 1978	17 32	17	−105	10	2.9	Osaka-Kyoto Border
10	78– 789	Aug. 22 1978	17 51	29	−28	10	2.9	Near Kyoto
11	78– 790	Aug. 22 1978	20 39	29	−28	10	3.4	Near Kyoto
12	78– 794	Aug. 23 1978	5 55	27	−20	20	2.7	Near Kyoto
13	78– 900	Sept. 25 1978	3 04	31	0	10	3.3	Shiga-Kyoto Border
14	78–1557	Dec. 25 1978	10 59	48	−28	10	2.8	Central Kyoto Pref.
15	78–1560	Dec. 26 1978	3 38	40	−78	20	3.1	Kyoto-Osaka Border
16	79– 125	Jan. 26 1979	2 45	34	−100	10	2.6	Nothern Osaka Pref.
17	79– 503	Apr. 9 1979	20 49	40	−61	20	2.9	Kyoto-Hyogo Border
18	79– 779	June 1 1979	7 33	35	−100	20	3.6	Osaka-Hyogo Border
19	79–1033	Aug. 18 1979	20 20	18	−160	10	2.3	Southern Kyoto Pref.
20	79–1186	Oct. 16 1979	7 45	42	5	10	4.9	NW Shiga Pref.
21	77–1391	Dec. 11 1977	22 39	28	149	0	2.7	Near Nara
22	78– 608	June 13 1978	22 42	22	145	0	2.7	Nara-Kyoto Border
23	78–1015*	Oct. 7 1978	13 18	23	142	10	3.7	Kyoto-Nara Border
24	78–1459	Dec. 5 1978	8 24	56	118	0	4.3	Central Mie Pref.
25	79– 520	Apr. 12 1979	13 59	24	127	10	4.3	Nw Mie Pref.
26	78– 219	Feb. 8 1978	3 33	28	107	60	3.8	Western Mie Pref
27	78–1187	Oct. 20 1978	16 00	39	123	60	3.5	Central Mie Pref.
28	79–1065	Sept. 12 1979	9 35	38	136	60	3.7	Mie-Nara Border
29	76– 584	Dec. 21 1976	8 04	82	−175	60	4.0	Southern Nara Pref.
30	78– 98	Jan. 16 1978	22 40	85	−173	70	3.5	Southern Nara Pref.
31	79– 265	Jan. 24 1979	12 35	83	−173	60	3.3	Southern Nara Pref.
32	79– 390*	Mar. 16 1979	10 36	85	−166	60	4.0	Wakayama-Nara Border
33	79– 988	July 31 1979	9 03	81	−160	70	4.0	Nothern Wakayama Pref.
39	79–1241	Nov. 13 1979	0 42	85	−166	70	4.8	Nara-Wakayama Border
40	76– 609	Dec. 27 1976	10 49	94	−145	0	4.0	Near Wakayama
41	77– 528*	Aug. 7 1977	4 27	98	−143	0	4.5	Near Wakayama
42	77– 615	Aug. 17 1977	0 32	103	−144	0	4.0	Near Wakayama
43	79– 555	Apr. 17 1979	20 26	112	−154	0	4.2	Central Wakayama Pref.
44	79–1261	Nov. 21 1979	8 36	83	−144	10	3.8	Wakayama-Osaka Border
45	77– 515*	Aug. 6 1977	2 44	96	71	50	4.3	Western Aichi Pref.
46	77– 605	Aug. 15 1977	21 03	71	71	20	3.7	Northern Mie Pref.
47	78–1064	Oct. 10 1978	3 10	72	53	10	3.8	SW Gifu Pref.
48	78–1079	Oct. 10 1978	4 02	71	54	10	3.6	SW Gifu Pref.
49	79– 15	Jan. 4 1979	16 21	54	79	40	3.2	Northern Mie Pref.
50	79– 252	Feb. 22 1979	4 18	56	121	0	3.2	Central Mie Pref.
51	79– 299	Mar. 1 1979	8 13	108	62	0	3.7	Gifu-Aichi Border
52	79– 417	Mar. 21 1979	4 53	63	85	40	3.2	Northern Mie Pref.

Table 1. Continued

No.	Event No.	Date	Time h m	Distance km	Azimuth N °E	Depth km	Magnitude	Region
53	76– 92	July 18 1976	15 30	150	−151	40	4.3	Kii Channel
54	76– 484*	Nov. 11 1976	6 05	97	141	40	4.4	S Coast of Mie Pref.
55	77– 859*	Sept. 8 1977	18 13	194	−131	20	4.6	Tokushima-Kochi Border
56	77–1463	Dec. 22 1977	5 11	123	158	50	4.0	S off Mie Pref.
57	78– 274	Feb. 21 1978	8 19	152	−130	50	4.0	Eastern Tokushima Pref.
58	78– 436	Apr. 9 1978	8 43	213	173	40	4.3	Off Kii Pen.
59	78– 522	May 15 1978	13 35	139	−138	60	4.4	Kii Channel
60	78– 635	June 20 1978	1 34	219	−160	60	4.3	Off Kii Pen.
61	76– 288	Sept. 21 1976	15 54	181	57	10	4.2	SW Nagano Pref.
62	76– 292*	Sept. 22 1976	3 04	172	49	0	4.3	Gifu-Nagano Border
63	78–1037	Oct. 9 1978	0 00	180	58	0	4.1	SW Nagano Pref.
64	79– 871	June 28 1979	21 29	181	56	10	4.0	SW Nagano Pref.
65	78– 416*	Apr. 3 1978	11 04	136	18	10	4.7	Near Fukui
66	79– 147	Jan. 30 1979	21 49	117	107	10	3.9	Atsumi Pen.
67	79–1182	Oct. 13 1979	16 30	95	−97	10	4.3	Southern Hyogo Pref.

* denotes the events, the envelopes of which are analyzed

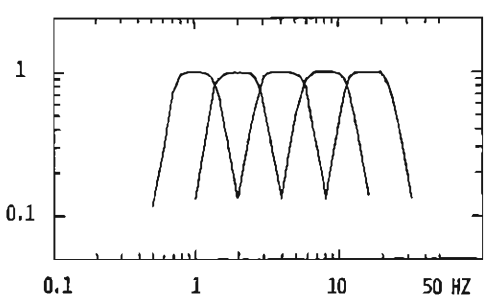

Fig. 2. Frequency response of band pass filters.

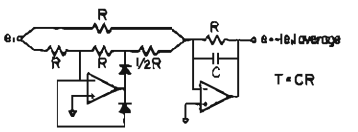

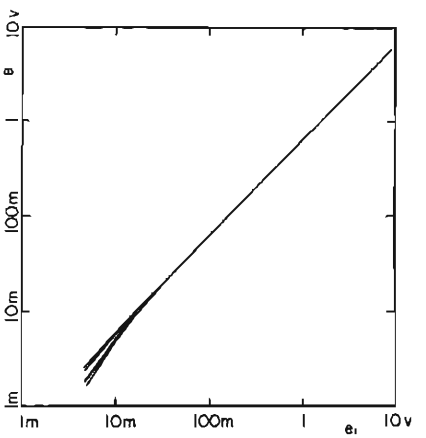

Fig. 3. Circuit diagram and amplitude response of ac meters used to generate rms amplitude of filtered traces of seismic coda parts.

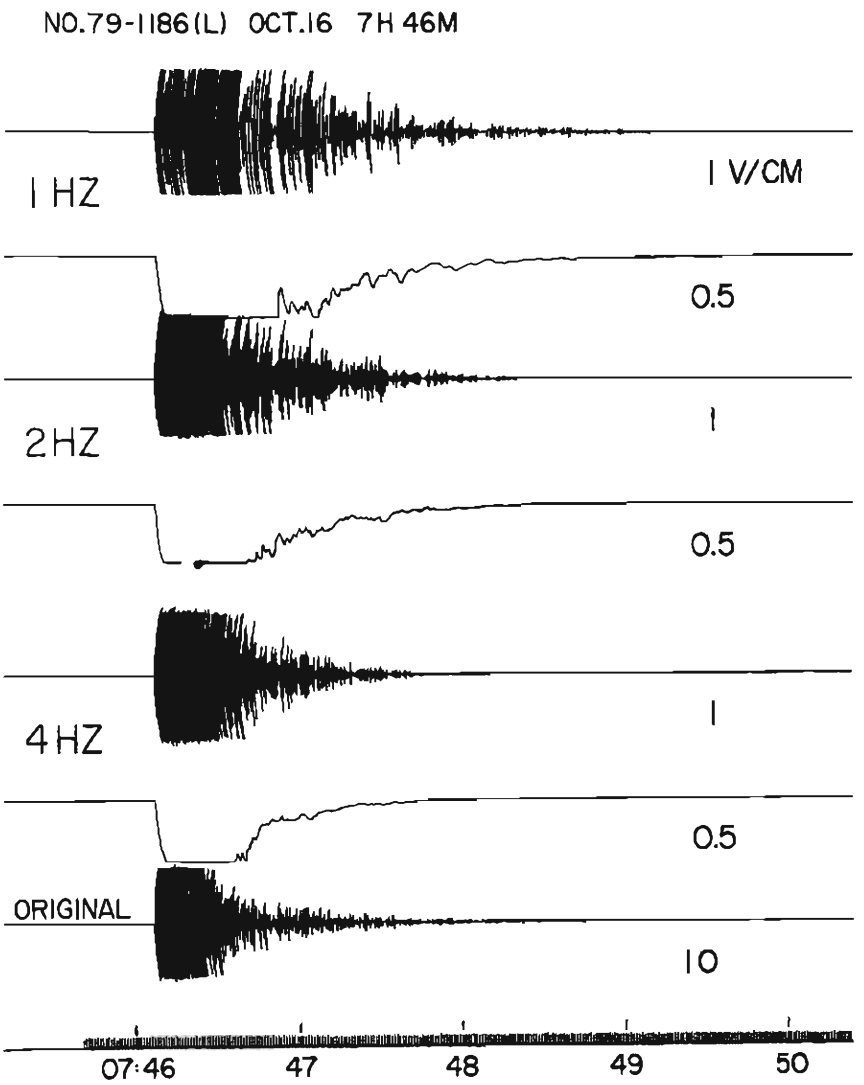

Fig. 4. Examples of band pass filtered traces of coda parts and their rms amplitudes generated by the ac meters shown in Fig. 3.

sampled for every time intervals corresponding to the time constant T of the integrators of the circuits. Therefore the analyzed time intervals and the number of the data points of $A(f, t)$ vary with the events as well as the filter channels. The total time intervals used for calculation range from 15 to 300 sec.

An example of the logarithmic rms amplitude $\ln A(f, t)$ and the curves fitted to $\ln A(f, t)$ with Eq. (2) is shown in Fig. 5. The log. amplitudes $A(f, t)$ are found to decay in the manner predicted by Eq. (2) although there is some amount of fluctuation of amplitudes.

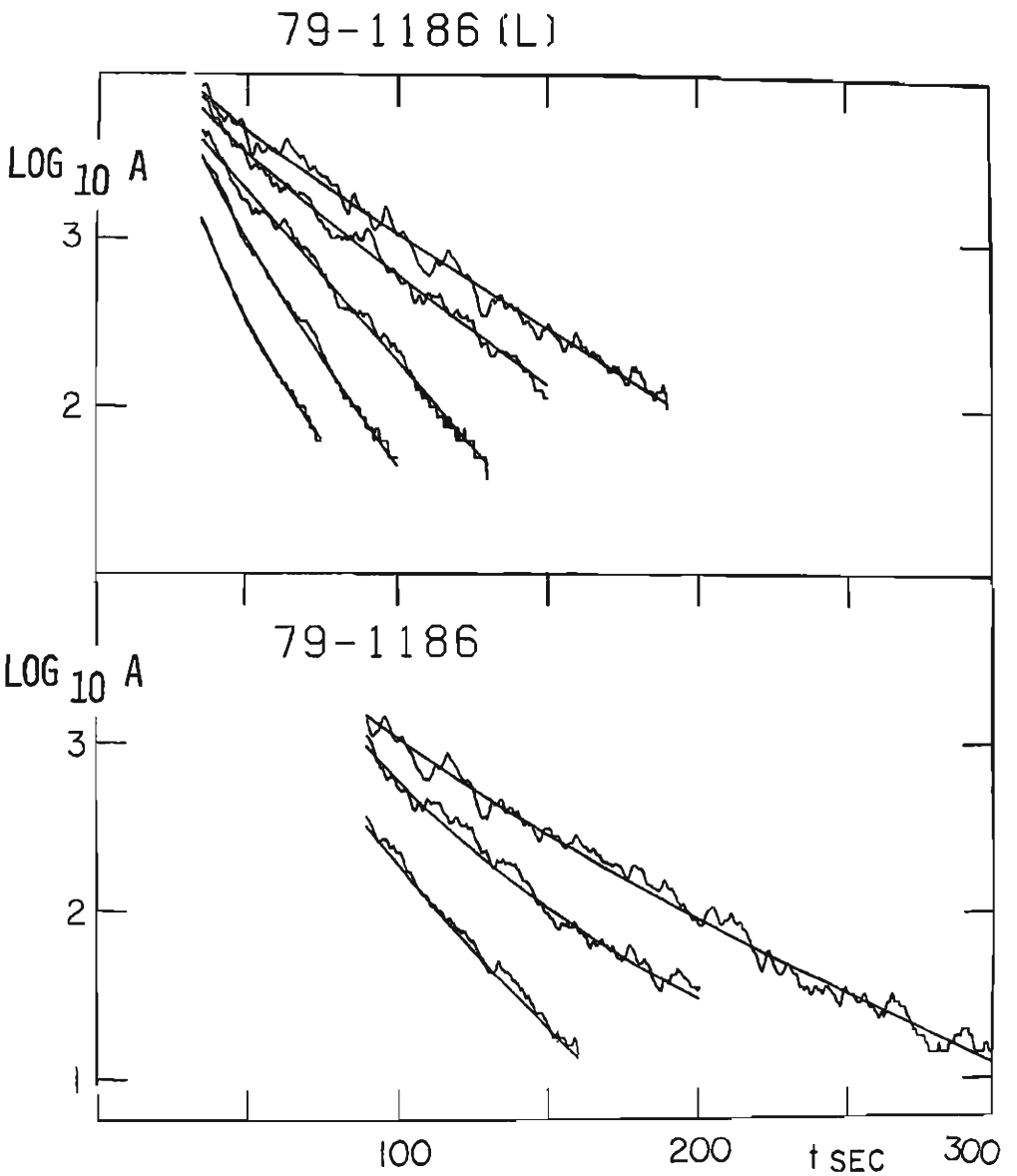

Fig. 5. Examples of logarithmic rms amplitudes $\ln A(f, t)$ and decay curves fitted with Eq. (2) by the least square method. NW Shiga Pref. Oct. 16 1979, 7 h 45 m, $\Delta=42$ km, $\varphi=$N5°E, $H=10$ km, $M=4.9$. Upper; low gain channel, lower; high gain channel.

3. Attenuation and fluctuation of coda

3-1. Coefficient a

An examination of the coefficient a in Eq. (2) is important to clarify the physical mechanism of wave scattering, which is considered to generate seismic coda as stated

previously. Unfortunately, however, the standard deviations of the calculated values of a are too large to discuss the values from the individual events. Therefore we may only derive the mean values of all events on the assumption that they are constant for events with different source conditions such as depth or hypocentral distance in our intervals of the lapse times (15~300 sec). The values of a range from 1 to 2 for all frequency bands although the deviations are rather large as listed in Table 2. This result is considered to suggest that the single scattering model of body wave is preferable to explain the coda parts rather than the other models described before. Therefore in the following, we may restrict our discussion of the coefficient b in Eq. (2) to the case of $a=1$ in solving the least square problems.

Table 2. The Values of the Coefficient a

f_0 HZ	1	2	4	8	16
a	1.2±0.7	2.1±1.0	1.9±0.6	1.6±1.3	1.2±1.4

3-2. Coefficient b

The values of coefficient b obtained with $a=1$ are shown in Fig. 6 for the values on the analyzed time intervals of each $A(f, t)$. They are conspicuous by two tendencies; the variation of b with the lapse time for all frequency bands, and the dependency on the frequency.

The values from $t<60$ sec show a tendency to be larger than those from the longer time intervals. In order to clarify the dependency of the values on the lapse time, they are estimated within some given time intervals for each $A(f, t)$ and are listed in Table 3. Although the deviations are large because of the short length of analyzed time intervals, it is very remarkable for all frequency bands that the values of b are large for the early time intervals and become smaller with time regularly to converge to some low constant values. The reasons for the dependency of b on the lapse time are considered in the following two ways. First, the predominant frequency of coda of the original seismogram decreases gradually with lapse time as is known as the coda dispersion[9]. The frequency contents of the filtered traces may vary with time because their band widths are relatively wide. Accordingly the attenuation of $A(f, t)$, which is remarkable in the decay characteristics of the higher frequency contents $(f_0+\Delta f)$ in the early lapse time, gradually becomes to be ruled by the lower values of the lower frequency contents $(f_0-\Delta f)$ as the time elapses. Secondly, the regions of the geological structures which are concerned with the generation and attenuation of the coda will become larger with time and the attenuation coefficient may converge to a low value for the deeper places in the earth.

To estimate the variation of frequency contents in $A(f, t)$ with time, the predominant frequencies of the traces from the band pass filters were read directly on the charts around the given lapse times. As are listed in Table 4, the predominant frequencies decrease only 10% from around the time $t=30$ sec to that of 50 sec. In the range $t>60$ sec there are no obvious differences in the predominant frequencies. The values of b become 1.3~1.8 times larger with 2 times increase of the frequency (octave change with each filter). Therefore the variations of b with time in any one pass band, estimated as 100% (Table 3), cannot be explained by a 10% change of

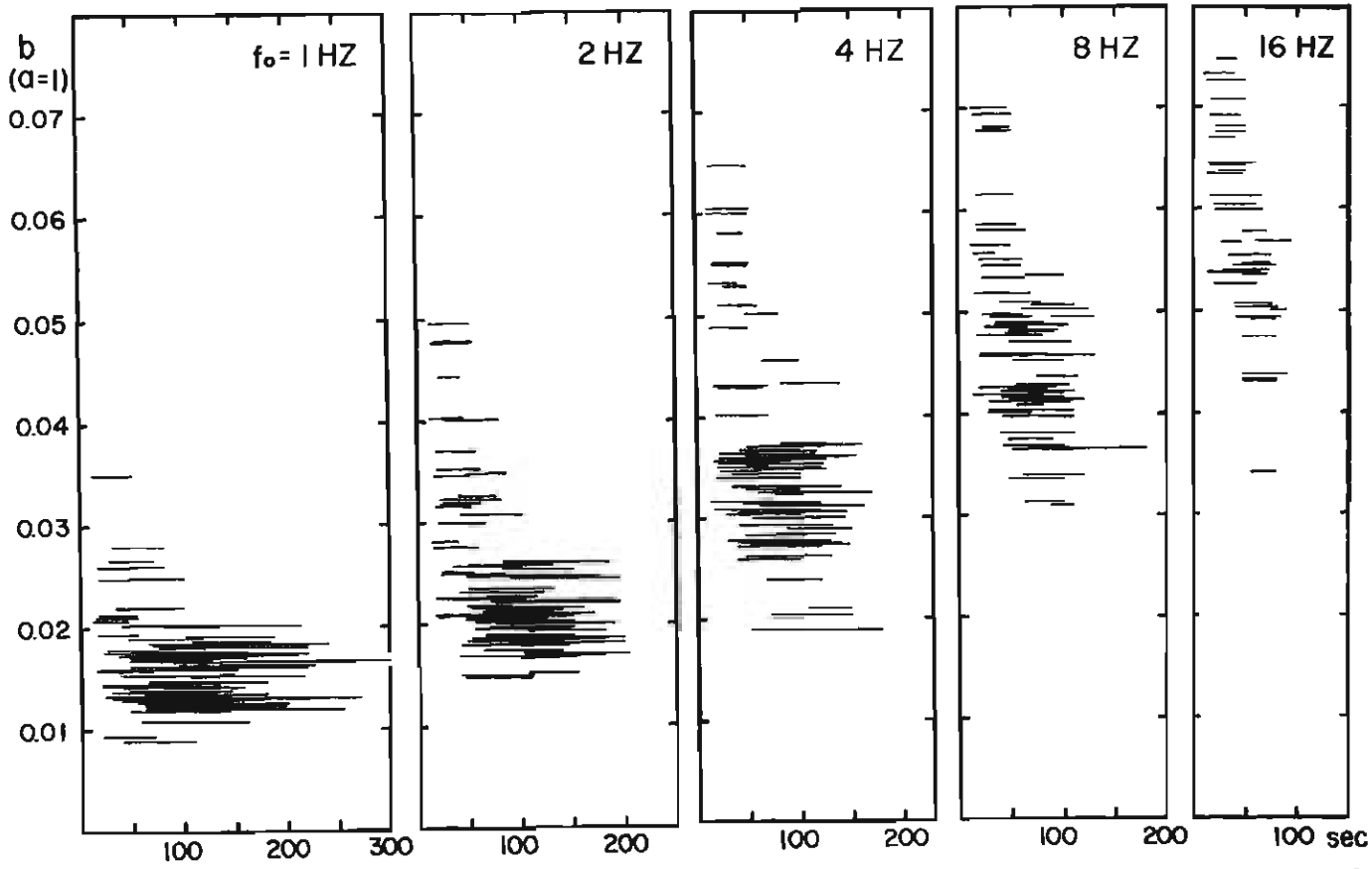

Fig. 6. Attenuation coefficient b obtained with each event under a condition $\alpha=1$. The value is displayed on each analyzed interval of the time.

Table 3. The Values of the Coefficient b within the Given Time Intervals $\times 10^{-3}$

f_0 \ t	15–45 SEC	20–60 SEC	40–90 SEC	60–120 SEC	80–150 SEC
1 HZ	2.37±1.65	1.96±1.18	1.79±0.68	1.37±0.47	1.37±0.41
1 HZ	3.95±1.16	3.37±1.40	2.02±0.75	2.02±0.50	1.97±0.53
4 HZ	5.68±0.66	4.62±0.67	2.92±0.53	3.04±0.29	3.10±0.42
8 HZ	5.62±0.59	4.75±0.53	4.07±0.34	3.78±0.45	
16 HZ	6.44±1.18				

Table 4. Predominant Frequencies of the Filtered Seismograms

f_0 \ t	30 SEC	50 SEC
1 HZ	1.24±0.11	1.09±0.10
2 HZ	2.12±0.24	1.98±0.22
4 HZ	4.13±0.47	3.76±0.37

frequency in the band (Table 4). For this reason the variation of the coefficient b with the lapse time is considered to reflect mainly the regional variation of the attenuation property of the medium.

The variation of the coefficient b with time may be consistent with the attenuation of the envelopes of the seismic coda in Garm region, where the coda in the frequency bands from 0.027 to 40 HZ cannot be fitted by a single curve of the form in Eq. (2) and is divided into a few segments, which can be fitted quite well with the curves of this type, but with different values of the attenuation coefficient for the different segments[8].

In this case we may give the following relation instead of Eq. (2);

$$\ln A(f, t)=\begin{cases} C-\ln t-b_1 t & \text{for} \quad t\leq t_c \\ C-\ln t-b_1 t_c-b_2(t-t_c) & \text{for} \quad t>t_c \end{cases} \tag{3}$$

where $a=1$ and t_c denotes the critical time at which the attenuation coefficient changes. Using the b values of $15\leq t\leq 45$ sec as the values of b_1 and those of $t\geq 100$ sec as b_2 in each frequency band, we can derive the critical time t_c by fitting Eq. (3) to the observed $\ln A(f, t)$. The values of t_c are estimated roughly as 45~50 sec for 1 and 2 HZ bands, and 40~45 sec for 4 and 8 HZ, respectively.

3–3. Turbidity coefficient g

The attenuation of the waves is considered to be caused by the intrinsic absorption of the medium and the scattering loss of energy by the heterogeneities in the medium. In the scattering theory of plane acoustic wave the attenuation of energy flow in a wave which passes through a layer of thickness L is given by the formula $\Delta I=\alpha IL$, from which we obtain the relation

$$\alpha=\frac{\Delta I}{IL} \tag{4}$$

for the scattering coefficient[13]. Under the assumption that the energy loss ΔI causes the fluctuation of the wave field, Nikolayev discussed the turbidity coefficient g of the forward scattering with experimental field data,

$$g=\frac{\Delta I}{IL}=\sigma^2(\ln A)/L \tag{5}$$

where σ^2 denotes the variance[14),15)].

In our case the coda parts of seismograms are characterized with some amounts of fluctuation of the amplitude and with the tendency of the increase of the fluctuations in the logarithmic amplitude with time as are observed in Fig. 5. These properties are consistent to the well-known and important ones of the scattered wave, showing the capability to discuss the turbidity for the seismic waves of coda parts with Eq. (5). In this case the process of generation of fluctuation is assumed to be as follows; a direct body wave from an earthquake source travels, suffering loss of energy by the forward scattering, to a point where scattered waves are generated backward, and the body waves generated by the backward scattering in turn come back to a observing point near the source, suffering the same forward scattering loss of energy as the original wave has been. The energy lost by the forward scattering in the going and coming propagations is observed as the fluctuation of the coda.

The values of $\sigma^2(\ln A)$ are calculated for each $\ln A(f, t)$ in some given time intervals using the mean values of $\ln A(f, t)$ obtained previously (i.e. the curves fitted with Eq. (2)), and are listed in Table 5a. Although they are extremely small and vary largely from event to event, it is remarkable that they become larger with the lapse time.

Table 5a. Fluctuation of the rms Amplitude of Coda Waves $\sigma^2(A_{rms})$ within the Given Time Intervals $\times 10^{-3}$

f_0 \ t	20–60 SEC	60–100 SEC	100–160 SEC	160–220 SEC
1 HZ	3.61±2.85	2.65±1.14	3.70±1.57	4.29±2.30
2 HZ	1.29±0.57	1.54±0.75	1.84±0.52	
4 HZ	0.96±0.52	1.26±0.67		
8 HZ	0.45±0.16	0.99±0.55		

Table 5b. Fluctuation of the Envelope of Coda Waves $\sigma^2(A_{env})$ within the Given Time Intervals $\times 10^{-2}$

f_0 \ t	60–100 SEC	100–160 SEC	160–220 SEC
1 HZ	5.85±1.51	7.19±1.68	8.12±2.35
2 HZ	10.4 ±3.8	6.86±2.81	
4 HZ	8.86±3.11		
8 HZ	6.26±1.48		

The small values of $\sigma^2(\ln A)$ and their dependency on frequency may be attributable mainly to the averaging effect of the integrators used for the construction of

the rms level of coda amplitude. To estimate the averaging effect of the integrators the envelopes of the filtered seismograms are analyzed to compare with the above result of the rms amplitude. The outputs of the band pass filters are digitized directly without the ac meters for some events selected arbitrarily (denoted by * in Table 1). The sampling frequencies of A–D conversion are 5 times the center frequency f_0 of each pass band. Using the envelopes of the coda we may derive the values of the variance $\sigma^2(\ln A_{env})$ as coda fluctuation. These are shown in Table 5b. The values from the envelopes are much larger than those of the rms amplitude and are rather constant with change of the pass bands. Therefore the small values and frequency dependency of $\sigma^2(\ln A_{rms})$ are attributed to the averaging effect of the circuits. The ratio of $\sigma^2(\ln A_{env})$ to $\sigma^2(\ln A_{rms})$ calculated with the same events for the same time intervals may be used as a quantitative estimation of the averaging effect. The mean ratios for the intervals from 60 to 100 sec are about 30 for 1 HZ, 60 for 2 and 4 HZ and 86 for 8 HZ, respectively. With these ratios and $\sigma^2(\ln A_{rms})$ we may estimate the amounts of fluctuation of the coda with which the turbidity coefficient g is derived from Eq. (5) under the assumption of no fluctuations at the earthquake source ($t=0$) and putting $L=V_s \cdot t=4 \cdot t$ km.

The results are listed in Table 6. The values of g are estimated to be $2\sim4\times10^{-4}$ km^{-1} for frequency range of $1\sim10$ HZ. It is noticable that the values decrease gradually with the lapse of time. The dependence of g on time is similar to that of the attenuation coefficient b on time, which is derived by quite a different way. This is very interesting as it may reflect the regional variation of turbidity in the earth. With the difference of the values of variance from the different time intervals we may estimate the turbidity coefficient of 0.95×10^{-4} km^{-1} for the deeper parts in the earth corresponding to lapse time intervals from about 50 to 200 sec.

Table 6. The Turbidity Coefficient g of Coda Waves for Given Time Intervals

$\times10^{-4}$km^{-1}

f_0 \ t	0–40 SEC	0–80 SEC	0–130 SEC	0–190 SEC
1 HZ	6.8±5.3	2.5±1.1	2.1±0.9	1.7±0.9
2 HZ	4.8±2.1	2.9±1.4	2.1±0.6	
4 HZ	3.4±2.0	2.4±1.3		
8 HZ	2.6±1.0	2.7±1.5		

Nikolayev et al. obtained the turbidity coefficient of the crust and the upper mantle[14),15)]. Their values are $2\sim5\times10^{-4}$ km^{-1} for frequency range of $6\sim12$ HZ with reflected P waves and $5\sim25\times10^{-4}$ km^{-1} for $2\sim12$ HZ with refracted P waves. Aki estimated the turbidity under Montana Lasa with teleseismic P waves[16)]. The value is 0.008 km^{-1} at 0.5 HZ. The turbidity coefficient obtained from the seismic coda are $1\sim2$ orders lower than those of the other field data except the values derived from reflected P waves.

Chernov showed in the scattering theory of acoustic waves that the scattering coefficient expressed by Eq. (4) depends on frequency for given acoustic random media[13)]. The values of g from the coda are rather constant for frequency.

The attenuation coefficient b may be expressed with the intrinsic absorption

$\pi f/Q$ and turbidity coefficient g with a multiplier 1/2 for conversion of the value for energy to that of amplitude as follows;

$$b = \frac{\pi f}{Q} + \frac{1}{2}\frac{g}{p}V_s \tag{6}$$

where p is a constant determined from the scattering mechanism. The value of p is 1 for the forward scattering and 0.5 for the forward and backward scattering for acoustic plane wave ($0.5 \leq p \leq 1$)[14]. In the case of the seismic waves of coda parts an assumption of plane wave is satisfactory for large lapse time and the mode conversion from S to P wave may be sufficiently small. Therefore using the values b and g obtained independently and putting $p=0.5$ and $V_s=4$ km/sec we may estimate the proportion of absorption and scattering loss in the attenuation of waves. The ratios of scattering loss to attenuation coefficient $(gV_s/2p)/b$ are listed in Table 7, in which the mean values of g for each time interval are used ($g=3.2\times10^{-4}$ for $t<60$ sec, $g=0.95\times10^{-4}$ for $t>50$ sec), because the values of g in Table 5 are rather constant with variation of frequency. The proportions of the scattering loss of energy in the attenuation are larger in the lower frequency range (up to 6%) than in the higher one due to the combined effects of the strong frequency dependency of attenuation coefficient b and nearly constant values of turbidity coefficient g. It becomes smaller than 3% for all frequency bands, although both of the values b and g become smaller for the large time. As the coda parts are considered to be generated by wave scattering caused by heterogeneities in the medium, it is suspected that the scattering loss of energy plays a relatively important role in the attenuation of coda. However, this idea does not agree well with the above result, which is obtained by the procedure based on the assumption of scattering loss of energy.

Table 7. The Rate of the Attenuation Due to the Scattering Loss of Energy to the Total Attenuation of Coda Waves $(gv_s/2p)/b$ with $g=3.2\times10^{-4}$ for $t=20$–60 and $g=0.95\times10^{-4}$ for $t>50$

f_0 \ t	t=20–60 SEC	t>50 SEC
1 HZ	6.0%	2.6
2 HZ	3.5	1.9
4 HZ	2.5	1.2
8 HZ	2.5	0.9
16 HZ	2.0	0.8

Fig. 7 shows the relation of the Q values to frequency with an assumption of no energy loss by scattering ($g=0$). The values estimated from the earlier time intervals ($t<60$ sec) may reflect the attenuation property of the shallow parts of the lithosphere. On the other hand the attenuation characteristics from later intervals ($t>50$ sec) may reflect the property of the deeper ones, as discussed previously.

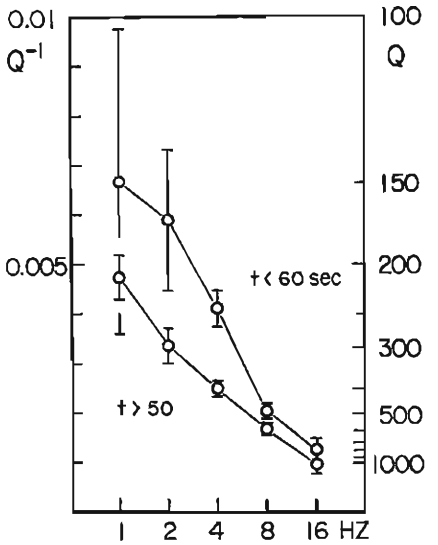

Fig. 7. Dependence of Q^{-1} values on frequency and lapse time. The variation of the values with different time intervals may reflect the variation of attenuation property in the lithosphere.

4. Conclusion

The attenuation parameters of the medium in the central Kinki district are discussed through the examination of the attenuation and fluctuation of the coda parts of seismograms from the local small earthquakes. The logarithmic rms amplitude of coda will converge fairly well to a general asymptotic decay curve of the form of Eq. (2), when the lapse time measured from the earthquake source time is larger than 3 times of the travel time of S wave ($t > 3 \cdot t_s$). The values of the coefficient a (the geometrical spreading factor) are $1 \sim 2$ for the frequency range from 1 to 20 HZ, suggesting that the coda parts may be regarded as the single scattered body waves caused by heterogeneities in the earth. The attenuation coefficient b obtained under the condition $a=1$, is larger for the early lapse time and converges to the low values with increase of time. This tendency is expressed fairly well by Eq. (3) with the critical time $t_c=40 \sim 50$ sec which may correspond to the layered model of attenuation parameters of the media.

The attenuation coefficient b for each time interval depends strongly on the frequency.

The turbidity coefficient g for the coda parts is derived from the fluctuation of the logarithmic rms amplitude independently of the attenuation of the coda. The value of g also decreases with time, showing the vertical variation of the turbidity in the earth. It is rather constant for the variation of the frequency, while the attenuation coefficient b depends on the frequency remarkably.

The amount of the scattering loss of energy is estimated with the turbidity coefficient g. The proportion of the scattering loss in the attenuation of coda is larger in the lower frequency range than in the higher ones. However, the attenuation is mainly attributable to the intrinsic absorption of the medium.

Two groups of the Q values for frequency range of $1 \sim 20$ HZ are obtained according to the different intervals of the lapse time. It is considered that one reflects mainly the attenuation property of the shallow regions of the lithosphere (or

the crust) and the other does that of deeper ones (or the upper mantle), respectively. The values of the first group are consistent with the data derived from the analyses of the shallow events with smaller magnitude than those of this study[3], and the values of the second group are consistent with the data from the deeper events (up to 160 km) with almost the same magnitude range[7].

Recently Kopnichev showed that seismic coda waves in a vertically isotropic medium are expressed by the form similar to Eq. (1) and that the geometrical spreading factor a takes a value $1 \sim 1.5$ in the case of a model in which the turbidity coefficient changes at the Moho boundary[17]. The attenuation properties discussed in this study seem to be also explained well by this model.

These observational results are very interesting in relation to the mechanism of generation and attenuation of coda parts of seismograms. Although this physical mechanism is not well understood, the attenuation property, that the amplitudes of coda waves from different earthquakes decay in the same manner independent of source locations and magnitudes, is very important to investigate the source spectra. Peak frequencies of body waves from micro-earthquakes ($M<3$) vary with source locations in relation with seismic activity in this region[18]. The spectral properties over a wide range of magnitude and in different regions may be examined by use of the coda spectra.

Acknowledgements

The author wishes to express his sincere thanks to Prof. Soji Yoshikawa of Kyoto University for his encouragement, and also to Dr. Tamotsu Furuzawa for his much valuable advice and encouragement in carrying out this work. The author is indebted to Messrs. Masao Nishi and Toshio Kobayashi for their helpful assistance with the observations and to Miss Kazue Segawa for her help.

The data processing was run on a FACOM M-130 at the Information Data Processing Center for Disaster Prevention Research, of the Disaster Prevention Research Institute of Kyoto University.

References

1) Soloviev, S. L.: Seismicity of Sakhalin, Bull. Earthquake Res. Inst., Tokyo Univ., Vol. 43, 1965, pp. 95–102.
2) Tsumura, K.: Determination of Earthquake Magnitude from Duration of Oscillation, Zisin, Second Series, Vol. 20, 1967, pp. 30–40 (in Japanese).
3) Aki, K and B. Chouet: Origin of Coda Wave: Source, Attenuation, and Scattering Effects, J. Geophys. Res., Vol. 80, 1975, pp. 3322–3342.
4) Востриков, Г. А.: Определение Сейсмического Момента Местных Землетрясений по Характеристикам Коды, Изв. АН СССР. Физика Земли, № 11, 1975, стр. 33–45.
5) Раутиан, Т. Г., В. И. Халтурин: Спектральные Свойства Коды Местных Землетрясений как Инструмент Исследования Очагового Излучения, докл. АН СССР. т. 226, № 3, 1976, стр. 566–569.
6) Chouet, B., K. Aki and M. Tsujiura: Regional Variation of the Scalling Law of Earthquake Source Spectra, Bull. Seism. Soc. Am., Vol. 68, 1978, pp. 49–79.
7) Tsujiura, M.: Spectral Analysis of the Coda Waves from Local Earthquakes, Bull. Earthquake Inst., Tokyo Univ., Vol. 53, 1978, pp. 1–48.

8) Rautian, T. G. and V. I. Khalturin: The Use of Coda for Determination of the Earthquake Source Spectrum, Bull. Seism. Soc. Am., Vol. 68, 1978, pp. 923–948.
9) Aki, K.: Analysis of the Seismic Coda of Local Earthquakes as Scattered Waves, J. Geophysic. Res., Vol. 74, 1969, pp. 615–631.
10) Раутиан, Т. Г., В. И. Халтурин, И. С. Шенгелия: Огибающие Сейсмической Коды и Оценка Магнитуд Землетрясений Кавказа, Изв. АН СССР. Физика Земли, № 6, 1979, стр. 22–29.
11) Clowes, R. M. and E. R. Kanasewich: Seismic Attenuation and the Nature of Reflecting Horizons within the Crust, J. Geophys. Res., Vol. 75, 1970, pp. 6693–6705.
12) Tsai, Y. B. and K. Aki: Simultaneous Determination of the Seismic Moment and Attenuation of Seismic Surface Waves, Bull. Seism. Soc. Am., Vol. 59, 1969, pp. 275–287.
13) Chernov, L. A.: *Wave Propagation in a Random Medium*, pp. 35–124, Dover edition, New York, 1967.
14) Nikolayev, A. V.: *Seismic Properties of Weakly Heterogeneous Media*, Izv., Earth Physics, (English translation), 1968, pp. 83–87.
15) Galkin, I. N. and A. V. Nikolayev: *Investigation of the Heterogeneity of the Earth's Crust and Upper Mantle by Recording the Amplitudes of Refracted Waves*, Izv., Earth Physics, (English translation), 1968, pp. 481–487.
16) Aki, K.: Scattering of P Waves under the Montana Lasa, J. Geophys. Res. Vol. 78, 1973, pp. 1334–1346.
17) Копничев, Ю. Ф.: Сейсмические Кода-Волны, "Наука" Москва 1978, стр. 5–29.
18) Furuzawa, T., K. Irikura and J. Akamatsu: Regional Variation of Body Waves' Spectra from Local Small Earthquakes Occurring in the Southern Parts of Kyoto, Zisin, Vol. 26, 1973, pp. 275–284 (in Japanese).